Structure and cytotoxic activity of sesquiterpene glycoside esters from *Calendula officinalis* L.: Studies on the conformation of viridiflorol

Michele D'Ambrosio[a,*], Alexandru Ciocarlan[a], Elisa Colombo[b], Antonio Guerriero[a], Cosimo Pizza[c], Enrico Sangiovanni[b], Mario Dell'Agli[b]

The sesquiterpene glycoside esters are responsible for cytotoxic effects of extracts of *C. officinalis*. Their structures were established by spectroscopic methods, chemical reactions and molecular mechanic calculations.

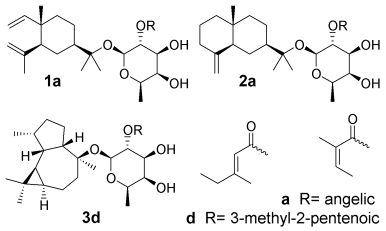

Structure and cytotoxic activity of sesquiterpene glycoside esters from *Calendula officinalis* L.: Studies on the conformation of viridiflorol.

Michele D'Ambrosio[a,*], Alexandru Ciocarlan[a,1], Elisa Colombo[b], Antonio Guerriero[a], Cosimo Pizza[c], Enrico Sangiovanni[b], Mario Dell'Agli[b]

[a] *Laboratory of Bioorganic Chemistry, Department of Physics, Università degli Studi di Trento, 38123 Trento, Italy*

[b] *Laboratory of Pharmacognosy, Department of Pharmacological and Biomolecular Sciences, Università degli Studi di Milano, 20133 Milan, Italy*

[c] *Dipartimento di Farmacia, Università degli Studi di Salerno, 84084 Fisciano (SA), Italy*

* Correspondence should be addressed to:
Tel: +39-0461-281509. Fax: +39-0461-281696.
E-mail address: michele.dambrosio@unitn.it

[1] Present address: Institute of Chemistry, Academy of Sciences of Moldova, str. Academiei 3, MD-2028, Chişinău, Republic of Moldova.

ABSTRACT

Topic applications of *Calendula officinalis* L. lipophilic extracts are used in phytotherapy to relieve skin inflammatory conditions whereas infusions are used as a remedy for gastric complaints. Such a different usage might be explained by some cytotoxicity of lipophilic extracts at gastric level but little is known about this. Therefore, we screened the CH_2Cl_2 extract from the flowers of *C. officinalis* by MTT and LDH assays in human epithelial gastric cells AGS. This bioassay-oriented approach led to the isolation of several sesquiterpene glycosides which were structurally characterized by spectroscopic measurements, chemical reactions and MM calculations. The conformational preferences of viridiflorol fucoside were established and a previously assigned stereochemistry was revised. The compounds **1a**, **2a** and **3d** showed comparably high cytotoxicity in the MTT assays, whereas the effect on LDH release was lower. Our study provides new insights on the composition of *C. officinalis* extracts of medium polarity and identifies the main compounds that could be responsible for cytotoxic effects at gastric level.

Keywords : *Calendula officinalis*; Asteraceae; Marigold; sesquiterpene glycoside; viridiflorol; ledol; α-elemol; β-eudesmol.

1. Introduction

Calendula officinalis L. is a plant widely cultivated for ornamental and medicinal purposes. *C. officinalis* is also being exploited as an industrial crop because of the high content of oil in its seeds (around 20%, of which about 60% is the unusual calendic acid) (Dulf et al., 2013).

Several reviews covering a variety of biological activities of *C. officinalis* have been recently published (Singh et al., 2011) and a multitude of phytochemical constituents have been identified (Muley et al., 2009). Many classes of chemical compounds occur in *C. officinalis* extracts, including volatile oils (Kaškonienė et al., 2011), carotenoids (Kishimoto and Ohmiya, 2009), fatty acids, triterpenoids, flavonoids, saponins (Szakiel et al., 2005) and polysaccharides. Reviews published on this topic (Andersen et al., 2010; Muley et al., 2009), do not report the presence of sesquiterpene glycosides and the studies on them have been neglected in comparison to the main components occurring in *C. officinalis*. Nonetheless, these glycosides are present in relatively significant amount. Several articles, appearing during the years 1987-2001, described the isolation and the structural elucidation of 24 new compounds (De Tommasi et al., 1990; Jakupovic et al., 1988; Marukami et al., 2001; Pizza and De Tommasi, 1988).

Clinical trials provide considerable evidence on the therapeutic effects of *C. officinalis* in the acceleration of wound healing and prevention of acute dermatitis (Cravotto et al., 2010). In fact, marigold apolar extracts are common ingredients of formulations for external use against local minor inflammations of the skin and mucosa (Campanini, 2003). The anti-inflammatory effect of these extracts is mainly due to the presence of fatty acid esters of pentacyclic triterpenols (Neukirch et al., 2004, 2005). Conversely, infusions from Marigold flowers have been traditionally consumed to relieve gastrointestinal inflammations including gastritis, ulcers and colitis (Campanini, 2003). The gastroprotective effect of these polar extracts might be due to the

presence of saponins (Yoshikawa et al., 2001). To sum up, apolar extracts are not recommended for ingestion whilst infusions do not contain the esterified triterpene alcohols.

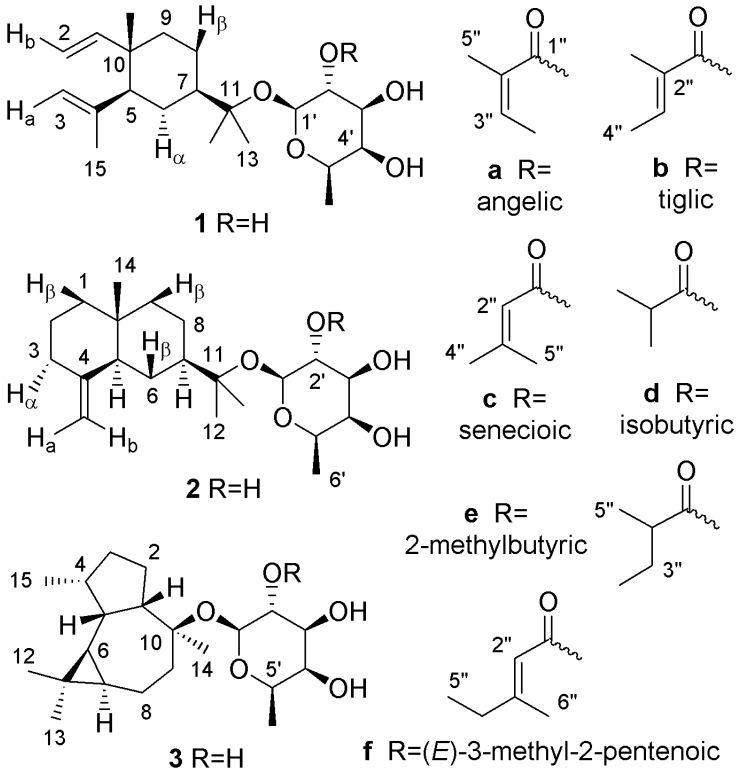

Fig. 1. Structural formulae of compounds **1**, **2**, **3** and their related ester moieties **a-f**.

In order to gain further information on the composition and gastric toxicity of apolar compounds from *C. officinalis*, we carried out the purification and identification of secondary metabolites guided by their assays for cytotoxicity in human gastric epithelial cells (AGS). The CH_2Cl_2 extract of flowers was subjected to separation by flash chromatography (FC) on silica gel thus obtaining 16 fractions **A-P** (Supplementary Fig. S1). Cytotoxicity in human gastric AGS cells of all fractions **A-P** from the crude extract was tested by 3-[4,5-dimethylthiazol-2-yl]-2,5-diphenyltetrazolium bromide (MTT) and the fractions **H** and **I** were found to be toxic. This result was partially confirmed by the LDH assay (Supplementary Fig. S2). The pentacyclic triterpenoid

esters occurred in the fractions **D**-**E** at low polarity. Consequently, the components of the fraction **H** at medium polarity were separated by high pressure liquid chromatography (HPLC) on a reversed phase C18 (RP18) column, thus leading out to the elucidation of one new α-elemol 11-*O*-β-D-(2'-acyl)-fucopyranoside, six (five of which are new) β-eudesmol 11-*O*-β-D-(2'-acyl)-fucopyranosides and five (among them one is new) viridiflorol 10-*O*-β-D-(2'-acyl)-fucopyranosides along with the two new α-elemol 11-*O*-β-D-fucopyranoside and β-eudesmol 11-*O*-β-D-fucopyranoside (Fig. 1).

2. Results and discussion

*2.1. Structural elucidation of compounds **1a** and **1***

Compound **1**a was isolated as white, amorphous powder; $[\alpha]^{25}_{D}$ –6.0 (*c* 0.17, $CHCl_3$). The ESI-MS spectrum had a molecular ion peak $[M-H]^-$ at *m*/*z* 449 (Supplementary Fig. S60). The compound **1a** was subjected to the reaction of acetylation (Subsection 4.6.1) and the diacetate product obtained was used for the HREIMS measurements. The molecular ion peak $[M]^+$ was measured at *m*/*z* 534.3187 (calcd. for $C_{30}H_{46}O_8$, 534.3192). Therefore the compound **1a** had molecular formula of $C_{26}H_{42}O_6$, implying 6 unsaturations. The 1D- and 2D-NMR spectra of compound **1a** (first RP18-HPLC peak) revealed the following substructural units: 1) an angelate group (Fig.1, substr. a) on the basis of ^1H-^1H couplings, the long-range correlation of the 3H-5" protons with the conjugated carboxyl C-1" and the NOESY maps of the olefinic H-3" with both the methyls 3H-4" and 3H-5", 2) a hexopyranose sugar (Fig.1, substr. 1) which corresponded to a β-fucose on the basis of its COSY maps and coupling constants, 3) a $C_{15}H_{26}O$ tertiary alcohol (Fig.1, substr. 1) which requires two double bonds and one cycle. According to ^1H-^{13}C long-range correlations (Table 2), the ring consisted of a cyclohexane that linked one methyl and a vinyl group at the quaternary carbon C-10, an isopropenyl group at the tertiary carbon C-5 and a

dimethyl carbinol at the tertiary carbon C-7. The relative configuration was established on the basis of the coupling constants of H-5 and H-7 and NOESY maps (Supplementary Fig. S58). Therefore, the structural formula of the sesquiterpene alcohol corresponds to α-elemol. Finally, the coupling constant of H-1' indicated the β-configuration of the glycosidic bond that occurred at C-11 as established by their ^{1}H-^{13}C long-range correlation. The chemical shift and the HMBC maps of H-2' indicated the position of the angelate ester (Supplementary Fig. S59).

Table 1.

^{1}H NMR (400 MHz, $CDCl_3$) spectroscopic data (δ in ppm, multiplicity, *J* in Hz) for compounds **1**, **1a**, **2**, **2a**, **3** and **3f**[a]

No.	**1**	**1a**[b]	**2**	**2a**[b]	**3**	**3f**[b]	**3f**[b,c]
1α	5.74, dd (17.2, 11.0)	5.78, dd	1.23, dd (13.0, 3.6)	1.18, dd	~1.92, m	~1.88, m	1.92, m
1β			~1.42, m /a	~1.44, m			
2α/a	4.83, m	4.87, m	~1.52, m	~1.58, m	~1.54, m	~1.60, m	1.62, m
2β/b	4.82, m	"	"	"	"	"	1.54, m
3α/a	4.74, m	4.78, m	1.91, br.q (11.0)	1.96, br.q	1.18, m	1.25, m	1.26, m
3β/b	4.51, br.s	4.54, br.s	2.22, br.d (13.3)	2.27, br.d	~1.72, m	~1.79, m	1.80, m
4					~1.88, m	~1.91, m	1.90, m
5	1.86, dd (12.2, 3.0)	1.88, dd	1.66, br.d (11.0)	1.69, br.d (12.2)	1.77, m (9.0, 4.6, 4.4)	1.67, m (9.0, 4.6, 4.4)	1.69, m
6α	~1.62, m	~1.61, m	1.63, br.d	1.64, dq (12.8, 2.7)	0.03, t (9.5)	0.03, t (9.5)	0.08, t
6β	1.35, q (12.0)	~1.35, q	1.06, q (12.7)	1.07, q (12.1)			
7	1.44, tt (12.0, 3.0)	~1.43, tt	1.44, tt	1.43, tt	0.52, td (9.5, 9.5, 7.6)	0.55, td (9.5, 9.5, 7.6)	0.58, ddd
8α	~1.61, m	~1.58, m	1.58, br.d	1.53, m	~1.50, m	~1.50, m	1.45, m
8β	~1.23, m	~1.18, m	1.21, dq (13.0, 3.3)	1.23, m	"	"	1.55, m
9α	~1.38, m	~1.37, m	~1.18, m	~1.24, m	~1.56, m	~1.55, m	1.60, m
9β	"	"	1.36, br.d (13.0)	1.40, br.d	~1.70, m	~1.74, m	1.73, m
12	1.14, s	1.15, s	1.14, s	1.15, s	0.91, s	0.84, s	0.90, s
13	1.17, s	1.22, s	1.15, s	1.21, s	0.94, s	0.96, s	0.98, s
14	0.92, s	0.94, s	0.62, s	0.66, s	1.10, s	1.18, s	1.18, s
15	1.63, br.s	1.67, br.s	4.62, br.s	4.66, br.s	0.84, d (6.7)	0.86, d (6.7)	0.88, d
(15b)			4.35, br.s	4.39, br.s			
1′	4.30, d (7.5)	4.60, d	4.30, d (7.5)	4.60, d	4.32, d (7.4)	4.61, d (7.9)	4.65, d
2′	3.38, dd (7.5, 9.6)	4.94, dd	3.37, dd (7.5, 9.6)	4.94, dd	3.37, dd (7.4, 9.5)	4.90, dd (7.9, 9.5)	5.00, dd
3′	3.46, dd (9.6, 3.4)	3.67, dd	3.44, dd (9.6, 3.4)	3.67, dd	3.43, dd (9.5, 3.4)	3.62, br.dd (9.5, 4.0)	~3.63, m
4′	3.58, dd (3.4, 1.1)	3.71, dd	3.56, dd (3.4, 0.7)	3.71, dd	3.55, dd (3.4, 0.5)	3.68, br.dd (4.0, 1.0)	~3.63, m
5′	3.52, qd (1.1, 6.5)	3.64, qd	3.50, qd (0.7, 6.6)	3.63, qd	3.48, qd (0.5, 6.5)	3.58, qd (1.0, 6.5)	~3.63, m
6′	1.22, d (6.5)	1.33, d	1.19, d (6.6)	1.32, d	1.18, d (6.5)	1.31, d (6.5)	1.24, d

[a]The assignments were based on COSY, edited HSQC and HMBC experiments. [b]For signals of ester chains see Table 3 or Experimental Section.
[c]Proton spectrum recorded in CD_3OD.

Table 2.

^{13}C NMR (100 MHz, $CDCl_3$) spectroscopic data (δ in ppm, multiplicity, HMBC maps) for compounds **1**, **1a**, **2**, **2a**, **3** and **3f**[a].

No.	**1**		**1a**[b]		**2**		**2a**[b]		**3**		**3f**[b]	
1	150.2,	14	150.1,	2, 14	41.1, t	14	41.0, t	14	54.4, d	14	53.8, d	14
2	109.6, t		109.6, t		23.37, t		23.4, t		25.5, t		25.5, t	
3	111.8, t		111.7, t		36.8 t	15	36.7, t	15	28.8, t	15	28.7, t	15
4	147.9, s	15	147.5, s	15	151.1, s	3, 5, 15b	150.8, s	3, 5, 15b	38.1, d	15	38.1, d	15
5	52.8, d	1, 3, 14, 15	52.6, d	3, 14, 15	49.9, d	6β, 14, 15	49.6, d	6β, 14, 15	39.6, d	15	39.4, d	15
6	28.2, t		27.7, t		24.8, t		24.4, t		22.2, d	12, 13	22.0, d	12, 13
7	48.1, d	12, 13	48.3, d	12, 13	48.2, d	12, 13	48.4, d	12, 13	28.5, d		28.8, d	12, 13
8	22.5, t		22.2, t		22.2, t		22.0, t		18.6, t		18.0, t	
9	39.9, t		39.7, t		41.8, t		41.7, t		37.0, t	14	38.1, t	14
10	39.6, s	1, 2, 14	39.6, s	1, 2, 14	35.8, s	14	35.8, s	14	82.1, s	14, 1'	81.5, s	14, 1'
11	80.0, s	12, 13, 1'	79.6, s	12, 13, 1'	80.2, s	12, 13, 1'	79.7, s	12, 13, 1'	18.5, s	6, 12, 13	18.4, s	6, 12, 13
12	23.2, q		22.5, q		23.42,		22.7, q		15.8, q		16.0, q	
13	24.4, q		25.0, q		24.3, q		24.8, q		28.5, q		28.6, q	
14	16.5, q		16.5, q		16.2, q		16.2, q		26.9, q		26.6 q	
15	24.6, q		24.5, q		105.0, t		105.2, t		16.1, q		16.1 q	
1′	97.0, d		95.0, d		97.0, d		94.8, d		96.5, d		94.4, d	
2′	71.5,[c] d		73.2, d		71.6,[c] d		73.2, d		71.6,[c] d		72.4, d	
3′	73.8, d		73.6, d		73.9, d		73.6, d		74.0, d		74.0, d	
4′	71.6,[c] d		71.8, d		71.5,[c] d		71.8, d		71.5,[c] d		71.9, d	
5′	70.2, d		69.8, d		70.1, d		69.8, d		70.1, d		69.6, d	
6′	16.3, q		16.4 q		16.2, q		16.4 q		16.1, q		16.4, q	

[a]The assignments were based on DEPT, edited HSQC and HMBC experiments. Long-range $^{1}H–^{13}C$ correlations are from the stated carbon to the indicated hydrogen(s). [b]For signals of ester chains see Table 3 or Experimental Section. [c]Assignments in the same column may be interchangeable;

The stereochemical elucidation of **1a** was achieved by chemical transformations. We subjected the crude fraction **H** to the condition of saponification and the mixture of reaction products to chromatography thus obtaining the pure compounds **1**, **2** and **3** (Subsection 4.4). The HRESI mass of compound **1** confirmed the structural formula (Supplementary Fig. S61). We tried to carry out the enzymatic hydrolysis of the saponificated compounds **1**, **2** and **3** but several enzymes failed to give the desired products. This prevented us from establishing the absolute configuration of α-elemol. Eventually, we subjected the products from the saponification

reaction, to acidic hydrolysis using a microwave assisted (Xiping and Yangde, 2008) procedure: the pure sugar gave a positive optical rotation thus proving it to be the (+)-D-fucose enantiomer. This result is in agreement with the absolute configuration of fucose that has been previously established either by X-ray crystallography (Takaoka et al., 1986) and chemical methods (Marukami et al., 2001).

Table 3.

NMR spectroscopic data of ester chains for compounds **2a**, **2b**, **2c**, **2d**, **2e**, and **2f**[a]

No.	**2a**		**2b**		**2c**		**2d**		**2e**		**2f**	
1″	167.7, s		168.1, s		166.9, s		167.3, s		177.5, s		177.4, s	
2″	127.0, s		128.0, s		115.3, d	5.68, m (1.3)	113.7, d	5.67, m (1.3)	34.1, d	2.58, m (7.0)	41.0, d	2.40, tq (6.9)
3″	139.1, d	6.11, qq (7.3, 1.4)	138.3, d	6.91, qq (7.1, 1.4)	158.6, s		164.0, s		18.8, q	1.18, d (7.0)	27.0, t	~1.70, m ~1.50, m
4″	15.8, q	2.00, dq (7.3, 1.5)	14.5, q	1.80, dq (7.1, 1.2)	27.5, q	1.90, d (1.3)	33.9, t	2.18, qd (7.4, 1.2)	19.2, q	1.19, d (7.0)	11.5, q	0.94, t (7.4)
5″	20.4, q	1.90, m (1.5, 1.4)	12.1, q	1.84, m (1.4, 1.2)	20.5, q	2.17, d (1.3)	12.1, q	1.07, t (7.4)			16.3, q	1.15, d (6.9)
6″							19.0, q	2.17, d (1.2)				

[a]Assignments were based on COSY, edited HSQC and HMBC experiments. ^{13}C NMR (100 MHz, $CDCl_3$) spectroscopic data (δ in ppm, multiplicity). ^{1}H NMR (400 MHz, $CDCl_3$) spectroscopic data (δ in ppm, multiplicity, *J* in Hz).

α-elemol is not very commonly isolated from natural sources, its 11-*O*-α-xylopyranoside was isolated as triacetate from *Iphiona scabra* D.C. (Abdel-Mogib et al., 1989) whereas its 11-*O*-α-D-arabinopyranoside was identified by spectral analysis in a mixture separated from *Lessingia glandulifera* A.Gray (Jolad et al., 1988). The more polar fraction **M** was also subjected to HPLC separation and furnished the pure compounds **1**, **2** and **3** (Subsection 4.3). This paper reports, for the first time, the characterization of the natural products α-elemol 11-*O*-β-D-fucopyranoside **1** and its 2'-*O*-angelate ester **1a** (Fig. 1).

*2.2. Structural elucidation of compounds **2a**–**2f** and **2***

Compound **2a** was isolated as white, amorphous powder; $[\alpha]^{25}_{D}$ –10.0 (*c* 0.4, $CHCl_3$). The ESI-MS spectrum had a molecular ion peak $[M-H]^-$ at *m*/*z* 449 (Supplementary Fig. S60). In the HREIMS measurements, the diacetate product of **2a** showed its ion peak [M]+ at *m*/*z* 534.3184 (calcd. for $C_{30}H_{46}O_8$, 534.3192). Therefore, **2a** (third RP18-HPLC peak) had molecular formula of $C_{26}H_{42}O_6$ and was the most abundant compound. Its 1D- and 2D-NMR spectra showed again the presence of a fucopyranose sugar esterified at C-2' by angelic acid and linked, by means of a β-glycosidic bond, to a tertiary alcohol which possessed a different structural formula because it implies one double bond and two cycles. Diagnostic HMBC correlation maps (Table 2) were observed: 1) from the exomethylene proton Hb-15, the methylene protons 2H-3 and the methyne proton H-5 to the olefinic singlet C-4, 2) from the methyl protons 3H-14 to the triplet C-1, the singlet C-10 and the doublet C-5, 3) from both the methyl protons 3H-12 and 3H-13 to the deshielded singlet C-11 and the doublet C-7, 4) from the anomeric proton H-1' to the same deshielded singlet C-11. Such a correlation pattern suggested a eudesmane arrangement of the carbon skeleton and precisely the β-eudesmol (Fig.1, substr. 2). The relative configuration was determined by the ^1H-^1H coupling constant values of H-5 and Hβ-6 and was also supported by NOESY maps (Supplementary Fig. S58). The product of saponification **2** was also isolated from the fraction **M** thus revealing itself as a new natural product. (Subsections 4.4 and 4.3). The compound **2a** has been previously reported from *Calendula persica* C.A. Mey. and our data were identical to the ones reported in the literature except for a few assignments of the ^{13}C chemical shifts (Jakupovic et al., 1988).). The authors did not measure the optical rotation of **2a** and we did not succeed in carrying out the enzymatic hydrolysis of **2**, so the absolute configuration remains undetermined. Nevertheless, practically all natural β-eudesmol is the (+)-(5S,7R,10R) enantiomer.

The second RP18-HPLC peak consisted of a mixture of β-eudesmol 11-*O*-β-D-fucopyranosides acylated at O-2' by tiglic / senecioic / isobutyric acids in the ratio 10:7:6 that we depicted as compounds **2b**, **2c** and **2d** respectively (Fig. 1). Two compounds from the fifth RP18-HPLC peak (Supplementary Fig. S1) revealed to be β-eudesmol fucosides acylated at O-2' by acids 2-methylbutyric **2e** and (*E*)-3-methyl-2-pentenoic **2f** (Fig. 1) in the ratio 1:4. The structures of minor compounds were unambiguously determined by spectroscopic analyses; their diagnostic NMR data and HREIMS measurements are reported in the experimental part. This is the first report on the isolation and structural elucidation of the natural products **2**, **2b**, **2c**, **2d**, **2e** and **2f**.

*2.3. Structural elucidation of compounds **3a–3d, 3f** and **3***

Compound **3f** was isolated as white, amorphous powder; $[\alpha]^{25}_{D}$ –6.8 (*c* 0.15, $CHCl_3$). The ESI-MS spectrum had a molecular ion peak $[M-H]^-$ at *m*/*z* 463 (Supplementary Fig. S60) and suggested a molecular formula of $C_{27}H_{44}O_6$. The HREIMS (Supplementary Fig. S60) of the esterified fucose cation observed from fragmentation of the diacetate derivative of **3f** (Subsection 4.6.3) as well as the HRESIMS (Supplementary Fig. S61) of the compound **3** (Subsection 4.4) fully supported the composition of **3f**. The structural formula of the pure compound **3f** (sixth RP18-HPLC peak) possesses the β-D-fucopyranose unit as indicated by its usual pattern of signals in the ^{1}H-NMR spectrum. Moreover, the proton-proton couplings, the Nuclear Overhauser effects of H-2" and the HMBC maps between the H-2', the H-2" and a conjugated carboxyl (Supplementary Fig. S59) proved the presence of a (*E*)-3-methyl-2-pentenoate ester (Fig. 1 substr. f) and its location on the sugar ring. Thus, the terpene moiety must be tricyclic and its proton spectrum showed three singlet methyls, one doublet methyl and two methyne protons resonating at a very high field (δ 0.03 and 0.55) which denoted a cyclopropane ring. The ^{1}H-^{13}C long-range correlations (Table 2) proved that two singlet methyls were geminal and linked to the

cyclopropane ring whereas one quaternary carbon joined the third singlet methyl and the anomeric oxygen of the fucose. All these spectroscopic data were reminiscent of an alloaromadendrol backbone as previously described in *Calendula* spp. extracts (Jakupovic et al., 1988; Pizza and De Tommasi, 1988).

The comparison of our proton chemical shifts with those from the literature revealed that they were identical (Jakupovic et al., 1988; Pizza and De Tommasi, 1988). However, one author (Jakupovic et al., 1988) proposed the (10*S*) configuration (i.e. viridiflorol) whereas the other author (Pizza and De Tommasi, 1988) assigned the epimeric (10*R*) (i.e. ledol). Careful scrutiny of the literature, revealed that the differentiation of epimeric C-10 alloaromadendrols cannot be definitely established by NOE results because the 3H-14 shows a strong enhancement of H-1 but none of the cyclopropyl protons in either case (Hirota et al., 1996). In addition, not only is the value of the specific optical rotation of ledol low, closely resembling that of viridiflorol, but its sign is dependent of the solvent (Thamapipol and Kündig, 2011). Ledol and viridiflorol can be differentiated by their characteristic melting points or, more easily, by the chemical shifts of the cyclopropyl protons (Kaplan et al., 2000). On the basis of known ^{1}H-NMR data (Fletcher et al., 2000; Jakupovic et al., 1988; Pizza and De Tommasi, 1988) and ours, this latter criterion seems to be also applicable to viridiflorol glycosides; thus, all the *Calendula* species biosynthesize (10*S*)-viridiflorol (Fig. 1). Finally, the structure of officinoside D was elucidated as the diglycoside derivative of 13-hydroxyledol (Marukami et al., 2001). The authors subjected it to enzymatic hydrolysis and stated that the spectroscopic data of the reaction product matched those for flourensadiol (Kingston et al., 1975). But flourensadiol was proven to consist of 12-hydroxyviridiflorol by X-ray crystallography (Pettersen et al., 1975). Therefore, the structure of officinoside D might need to be revised.

The (10*S*)-viridiflorol has also been identified as its 10-*O*-β-D-quinovopyranoside (Jakupovic et al., 1988) and 10-*O*-α-rhamnopyranoside (Fletcher et al., 2000). The fraction collected at t_R=28.0 min (forth RP18-HPLC peak) contained two minor compounds which were identified as the new viridiflorol 10-*O*-β-D-(2'-tigloyl)-fucopyranoside **3b** and the known viridiflorol 10-*O*-β-D-(2'-senecioyl)-fucopyranoside **3c** (Jakupovic et al., 1988) in the ratio of 4:5 (Supplementary Fig. S1). Two additional compounds from the fifth RP18-HPLC peak (Supplementary Fig. S1) were characterized as the known viridiflorol 10-*O*-β-D-(2'-isobutyryl)-fucopyranoside **3d** and viridiflorol 10-*O*-β-D-(2'-angeloyl)-fucopyranoside **3a** (De Tommasi et al., 1990). Only diagnostic NMR data of minor compounds are reported in the experimental part. The compound **3,** obtained by saponification of **3a** and by separation of fraction **M** (Subsections 4.4 and 4.3) was previously reported as a natural product. The composition of the fraction **I** was similar to that of fraction **H**.

*2.4. MM calculation of compound **3f***

The most stable conformation of (10*R*)-ledol was calculated by a molecular mechanic (MM) software thus establishing that the cycloheptane ring adopts a boat like conformation (Freeman et al., 2008) with the 3H-14 in an equatorial orientation (Kaplan et al., 2000). Similarly, we undertook the MM calculation of the lowest energy conformer of (10*S*)-viridiflorol. The outcome of MM calculations for (10*S*)-viridiflorol proved that the 3H-14 still occupies an equatorial position but the cycloheptane ring has a chair like conformation (Freeman et al., 2008). This is consistent with the lack of NOE interactions between 3H-14 and the cyclopropyl protons. Since it was unequivocally established that the fucose moiety possessed the (+)-D stereochemistry, we further extended the MM calculations to compounds **3** and **3f**. Assuming that we had the (10*S*)-viridiflorol enantiomer in hand and by the sequential application of the dihedral driver routine to

the bonds C10-O10, O10-C1', C2'-O2', and C1"-C2", we obtained the lowest energy conformer which is shown in the Figure 2.

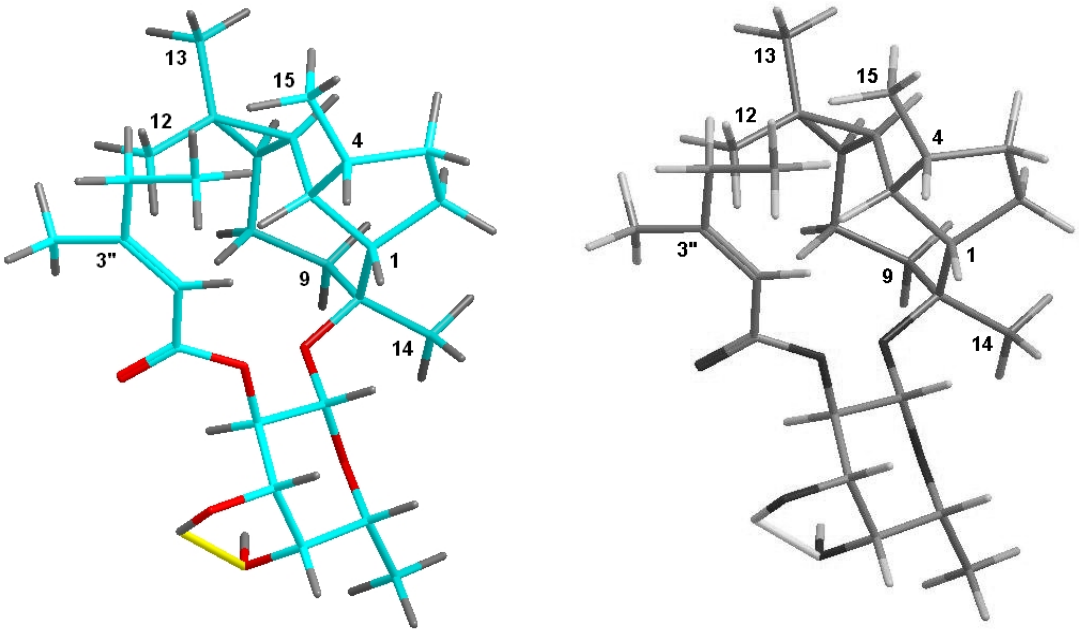

Fig. 2. Molecular mechanics calculated lowest-energy conformer of compound **3f**.

This preferred conformation prompts the following comments: 1) the pyranose ring turns its α-side toward the cyclopentane ring and the H-1' stays between H-1 and 3H-14, 2) the 3H-6' is directed outwards and the ester chain reaches out over the cyclopropane. Such an arrangement is supported by the intense NOEs of H-1' with both H-1 and 3H-14 as well as by the weak though noticeable NOEs of H-2" with both H-5 and 3H-12 (Supplementary Fig. S59). The presence of a carboxylic acid bound to the C-2' hydroxyl in **3**, causes shifts of the NMR resonances for H-5, H-6, H-7, 3H-12, 3H-13 and 3H-15 which with the unsaturated ester chains are mostly located up-field while with the saturated ones are found down-field (Pizza and De Tommasi, 1988). This effect may be attributed to the anisotropic shielding cone of the conjugated C=C double bond.

The difference between the resonances Δ(δsat—δunsat), calculated from our NMR data acquired in $CDCl_3$, clearly show that the highest shielding effect applies to 3H-12.

We also drew the compounds **3** and **3f** with the (10*R*)-viridiflorol enantiomer and calculated the lowest energy conformer. In this minimized structure, the ester chain again reached out over the cyclopropane but the H-1' stayed between 3H-14 and Ha-9. This arrangement is inconsistent with the experimental NMR data thus pointing out that **3** is constituted by the (10*S*) enantiomer of viridiflorol. In conclusion, MM calculations agree with NMR data and the most stable conformation shown in Figure 2 matches the perspective drawing previously obtained by X-ray crystallography (Takaoka et al., 1986).

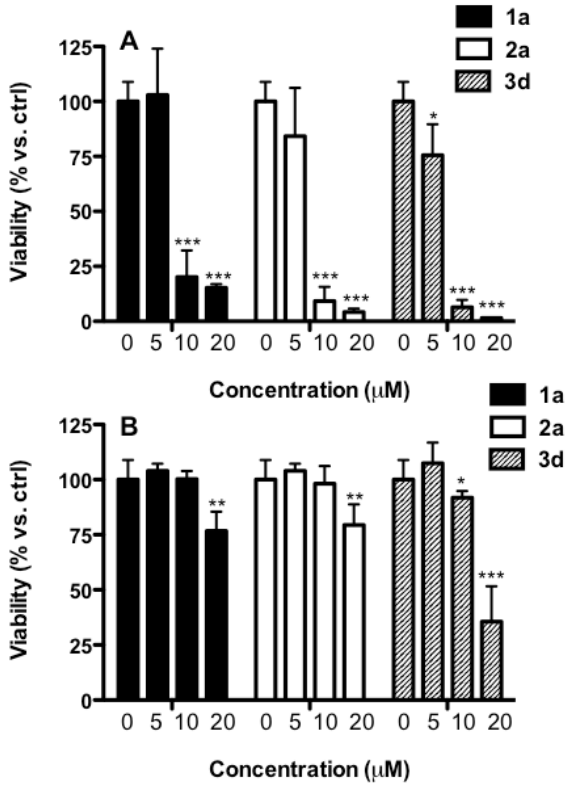

Fig. 3. Cytotoxicity of pure compounds **1a**, **2a** and **3f** from fraction **H** by MTT test (panel A, 5-20 μM) and by LDH assay (panel B, 5-20 μM). Triton-X100 1% was used as positive control, showing about 100% and 90% inhibition of cell viability for MTT and LDH assays, respectively.

*2.5. Cytotoxicity of **1a**, **2a** and **3f** by MTT and LDH assays*

In order to identify the constituents responsible for the cytotoxic effect seen with fraction **H**, the pure compounds **1a**, **2a** and **3f** were also assayed by MTT test. Individual compounds **1a**, **2a**, and **3f** already showed high cytotoxicity at 10 μM (83%, 92% and 99%, respectively), thus suggesting these compounds are the most responsible for the cytotoxicity of the fraction **H**. The IC_{50} were as follows: **1a** = 6.46 ± 0.011 μM; **2a** = 5.42 ± 0.022 μM; **3f** = 5.78 ± 0.96 μM (mean ± S.D.). The three individual compounds possessed lower cytotoxicity in the LDH assay (24%, 21% and 65% at 20 μM, respectively), thus mirroring the effect previously shown by **H** and **I** fractions. IC_{50} value of the most toxic compound **3f** was 15.4 ± 0.05 μM (mean ± S.D.). Specifically, the extracts and pure compounds showed higher toxicity in the MTT than in the LDH assay. Indeed, it has been previously revealed that MTT assay gives greater sensitivity than the LDH assay; this could be due to the generation, by toxic compounds, of reactive oxygen species within the mitochondria leading to damage of mitochondrial components and giving signs of toxicity earlier than LDH release (Fotakis and Timbrell, 2006).

In order to gain further information about the stability of these compounds in the stomach, the CH_2Cl_2 extract was subjected to *in vitro* gastric digestion, thus mimicking the gastric environment. The reactivity of the components was assessed by HPLC and most of the sesquiterpenes glycosides could still be detected after the treatment. Such a result indicated that these molecules are present in an unaltered form in the stomach. However, the metabolic fate and bioavailability of these compounds after passage through the stomach is still unknown.

3. Concluding Remarks

Herbal medicines represent a promising source of lead compounds for drug development and also benefit from easy accessibility and low-cost availability. However, the past and future major challenge of herbal medicines is to demonstrate evidence-based therapeutic use. Our paper provides new insights on the components of medium polarity of *C. officinalis* extracts and identifies the main compounds that could be responsible for cytotoxic effects at gastric level, if highly concentrated. Therefore, varieties of *C. officinalis* with low content of sesquiterpene glycosides should be selected for cultivation for medicinal purposes.

4. Experimental

4.1. General experimental procedure

Optical rotations were measured on a Bellingham+Stanley ADP 440 polarimeter. 1D and 2D NMR spectra were recorded on a Bruker Avance 400 spectrometer at 400 MHz (^{1}H) and 100 MHz (^{13}C) in 5 mm BBI probe. Chemical shifts are reported in ppm (δ), using the residual solvents signals as internal reference ($CDCl_3$ = 77.0, $CHCl_3$ = 7.26 and CD_2HOD = 3.31). Coupling constants (*J*) are in Hz. ^{1}H and ^{13}C NMR assignments were supported by ^{1}H,^{1}H COSY, $^{1}J_{CH}$ (HSQC), $^{n}J_{CH}$ (HMBC) and NOESY experiments. Selected HMBC (blue arrow, H → C) and key NOESY (red line) correlations of compounds **1**, **2** and **3** are shown in the Supplementary data (Fig. S58); full HMBC and NOESY correlations for all compounds are given in the Supplementary data (Fig. S59). Electrospray ionization mass spectra (ESIMS) were recorded on a Bruker Esquire_LC multiple ion trap; capillary voltage 4000 V, nebulizing pressure 30.0 psi, drying gas flow 7 mL/min, temperature 300 °C. The HRESIMS detection was performed using a LTQ-Orbitrap hybrid mass spectrometer (Thermo Fisher Scientific, Bremen, Germany) fitted

with an electrospray source (ESI) operating in positive ionization mode (Supplementary Fig. S61). Electron impact mass spectra (EIMS, HREIMS) were recorded on a Kratos MS80 spectrometer with home-built data system; electron ionization at 70 eV, *m/z* (rel. %). For flash chromatography commercial silica gel Merck Kieselgel 60 (70-230 mesh) and Merck RP 18 LiChroprep (40-65 μm) was used. Precoated silica gel plates Merck Kieselgel 60 PF254 were used for analytical TLC. HPLC separations were performed on a Merck Hitachi system equipped with an L7100 pump, an L7400 UV detector, a D7500 integrator and a manual Rheodyne injector. The following HPLC columns and methods were used: i) RP18 Synergi Hydro column (150×10 mm, 4 μm particle size, 80 Å pore size; Phenomenex, Torrance, CA, USA), 5.0 mL/min, λ=254 nm; for the fraction H the eluents were CH_3CN (A) and $CH_3CN–H_2O$ (50:50) (B) and the gradient was changed linearly from 0% to 85% A in 45 min; for the fraction M the eluents were CH_3CN (A) and $CH_3CN–H_2O$ (40:60) (B) and A was applied in the gradient of 0% at t=0, 0% at t=10, 37% at t=30, 85% at t=31, 85% at t=45, 100% at t=46 min; for the saponificated mixture the eluents were MeOH–H_2O (75:25). ii) Allure Biphenyl column (150×4.6 mm, 5 μm particle size, 60 Å pore size; Restek, Bellefonte, PA, USA), 1.0 mL/min, λ=254 nm; the eluents were CH_3CN (A) and $CH_3CN–H_2O$ (50:50) (B) and A was applied in the gradient of 0% at t=0, 23% at t=30, 85% at t=35 min; iii) Luna CN column (150×4.6 mm, 3 μm particle size, 100 Å pore size; Phenomenex, Torrance, CA, USA), 0.8 mL/min, λ= 210, 254, 290 nm; the eluents were *n*-hexane (A) and *i*-PrOH (B) and B was applied in the gradient of 1% at t=0, 1% at t=5, 10% at t=35, 10% at t=50 min. The microwave-assisted hydrolysis experiments were performed with a Discover SP system (CEM, USA). Molecular mechanics (MM) calculations were carried out with the PCModel v9.100 computer program. Lactate dehydrogenase (LDH) Cytotoxicity Detection Kit was provided by Takara Bio Inc. (Otsu, Shiga, Japan). 3-(4,5-dimethylthiazol-2-yl)-2,5-

diphenyltetrazolium bromide dye (MTT) and reagents for gastric digestion were provided by Sigma-Aldrich (Milan, Italy).

4.2. Plant material

Dry flowers of *C. officinalis* (variety Calypso Orange Florensis) were obtained and extracted as previously described (Neukirch et al., 2004). A voucher specimen (N. 20040929) is deposited at the Laboratory of Bioorganic Chemistry.

4.3. Extraction and isolation

A portion of the extract was subjected to FC on silica gel (Ø7 cm × 10 cm), gradually increasing the eluent polarity from *n*-hexane−EtOAc (95:5) to absolute ethyl acetate (300 mL fraction volume) and then washing with acetone (Supplementary Fig. S1). This procedure afforded 16 fractions. The fraction H (0.78 g) was collected with *n*-hexane−EtOAc 3:7; a portion (~100 mg) was submitted to HPLC on the RP18 column to yield six fractions that contained the following compounds: **1a** (t_R=24.0 min, mg 5.8); **2b**+**2c**+**2e** (t_R=25.1 min, mg 3.6), **2a** (t_R=26.9 min, mg 22.6), **2a**+**3b**+**3c** (t_R=28.0 min, mg 2.3), **3e**+**3a**+**2d**+**2f** (t_R=29.2 min, mg 14.0), **3d** (t_R=31.7 min, mg 9.8). The peaks at t_R=28.0 and 29.2 min were further separated by HPLC on the biphenyl column to yield respectively: two fractions containing **3b**+**3c** (t_R = 21.9 min, mg 1.0), **2a** (t_R=23.5 min, mg 0.6) and three fractions containing **3e** (t_R=25.5 min, mg 0.8), **3a** (t_R=27.8 min, mg 3.1), **2d**+**2f** (t_R=29.4 min, mg 4.4). Fraction M (0.10 g) was collected with acetone; a portion (~50 mg) was submitted to HPLC on RP 18 column with a gradient of CH_3CN in H_2O to yield several fractions. The fractions that interested us, contained the following compounds: **1** (t_R=16.5 min, mg 3.3), **2** (t_R=18.1 min, mg 5.7), **3** (t_R=21.8 min, mg 10.9).

4.3.1. Compound (**1**)

White, amorphous powder; $[\alpha]^{25}_{D}$ +3.5 (*c* 0.28, isopropanol); ^{1}H NMR ($CDCl_3$, 400 MHz) see Table 1; ^{13}C NMR ($CDCl_3$, 100 MHz) see Table 2. HR-ESI-MS (positive mode): *m/z* 391.2459 $[M+Na]^+$; (calcd. for $C_{21}H_{36}O_5Na$, 391.2455).

4.3.2. Compound (**1a**):

White, amorphous powder; $[\alpha]^{25}_{D}$ –6.0 (*c* 0.17, $CHCl_3$); ^{1}H NMR ($CDCl_3$, 400 MHz) see Table 1 and δ 6.10 (1H, qq, J = 7.3, 1.4 Hz, H-3"), 2.00 (3H, dq, J = 7.3, 1.5 Hz, H-4"), 1.89 (3H, m, H-5"); ^{13}C NMR ($CDCl_3$, 100 MHz) see Table 2 and δ 169.5 (C, C-1"), 126.7 (C, C-2"), 139.0 (CH, C-3"), 15.8 (CH_3, C-4"), 20.3 (CH_3, C-5"); ESI-MS (positive mode): *m/z* 473 $[M+Na]^+$; MS^2 of $[M+Na]^+$: *m/z* 269 $[M+Na\text{-}C_{15}H_{24}]^+$; MS^3 of $[M+Na]^+ \rightarrow [M+Na\text{-}C_{15}H_{24}]^+$: *m/z* 251 $[M+Na\text{-}C_{15}H_{24}\text{-}H_2O]^+$. ESI-MS (negative mode): *m/z* 449 $[M-H]^-$; MS^2 of $[M-H]^-$: *m/z* 367 $[M\text{-}H\text{-}C_5H_6O]^-$; MS^3 of $[M-H]^- \rightarrow [M\text{-}H\text{-}C_5H_6O]^-$: *m/z* 145 $[M\text{-}H\text{-}C_5H_6O\text{-}C_{15}H_{26}O]^-$.

4.3.3. Compound (**2**)

White, amorphous powder; $[\alpha]^{25}_{D}$ +33.3 (*c* 0.72, isopropanol); ^{1}H NMR ($CDCl_3$, 400 MHz) see Table 1; ^{13}C NMR ($CDCl_3$, 100 MHz) see Table 2. HR-ESI-MS (positive mode): *m/z* 391.2458 $[M+Na]^+$; (calcd. for $C_{21}H_{36}O_5Na$, 391.2455).

4.3.4. Compound (**2a**)

White, amorphous powder; $[\alpha]^{25}_{D}$ +10.0 (*c* 0.4, $CHCl_3$); ^{1}H NMR ($CDCl_3$, 400 MHz) see Tables 1 and 3; ^{13}C NMR ($CDCl_3$, 100 MHz) see Tables 2 and 3; ESI-MS (positive mode): *m/z* 473 $[M+Na]^+$; MS^2 of $[M+Na]^+$: *m/z* 269 $[M+Na\text{-}C_{15}H_{24}]^+$; MS^3 of $[M+Na]^+ \rightarrow [M+Na\text{-}C_{15}H_{24}]^+$: *m/z* 251 $[M+Na\text{-}C_{15}H_{24}\text{-}H_2O]^+$. ESI-MS (negative mode): *m/z* 449 $[M-H]^-$; MS^2 of [M-

H]$^-$: *m/z* 367 [M-H-C_5H_6O]$^-$; MS^3 of [M-H]$^-$ → [M-H-C_5H_6O]$^-$: *m/z* 145 [M-H-C_5H_6O-$C_{15}H_{26}O$]$^-$.

4.3.5. Compound (**2b**)

Solid mixture; ^{1}H NMR ($CDCl_3$, 400 MHz) see Table 3 and δ ~1.43 (1H, m, H-1β), 1.18 (1H, dd, H-1α), ~1.58 (2H, m, H-2), 2.28 (1H, brd, H-3β), 1.96 (1H, brq, H-3α), 1.68 (1H, brd, H-5), 1.66 (1H, dq, H-6α), 1.05 (1H, q, H-6β), ~1.42 (1H, tt, H-7), ~1.53 (1H, m, H-8α), ~1.23 (1H, m, H-8β), 1.40 (1H, brd, H-9β), ~1.22 (1H, m, H-9α), 1.15 (3H, s, H-12), 1.21 (3H, s, H-13), 0.65 (3H, s, H-14), 4.67 (1H, brs, H-15a), 4.36 (1H, brs, H-15b), 4.61 (1H, d, H-1'), 4.90 (1H, dd, H-2'), 3.67 (1H, dd, H-3'), 3.71 (1H, dd, H-4'), 3.63 (1H, qd, H-5'), 1.33 (3H, d, H-6'); ^{13}C NMR ($CDCl_3$, 100 MHz) see Table 3. ESI-MS (positive mode): *m/z* 473 [M+Na]$^+$; MS^2 of [M+Na]$^+$: *m/z* 269 [M+Na-$C_{15}H_{24}$]$^+$. EIMS of the diacetate: *m/z* 534 [M]$^{+\bullet}$ (0.3), 313 [M-$C_{15}H_{25}O$]$^+$ (16), 204 [M-$C_{15}H_{22}O_8$]$^{+\bullet}$ (24), 83 (100). HREIMS: *m/z* 534.3189 (calcd for $C_{30}H_{46}O_8$, 534.3193), 313.1290 (calcd for $C_{15}H_{21}O_7$, 313.1287).

4.3.6. Compound (**2c**)

Solid mixture; ^{1}H NMR ($CDCl_3$, 400 MHz) see Table 3 and δ 1.15 (3H, s, H-12), 1.21 (3H, s, H-13), 0.66 (3H, s, H-14), 4.67 (1H, brs, H-15a), 4.40 (1H, brs, H-15b), 4.56 (1H, d, H-1'), 4.81 (1H, dd, H-2'), 1.33 (3H, d, H-6'); ^{13}C NMR ($CDCl_3$, 100 MHz) see Table 3. ESI-MS (positive mode): *m/z* 473 [M+Na]$^+$; MS^2 of [M+Na]$^+$: *m/z* 269 [M+Na-$C_{15}H_{24}$]$^+$. EIMS and HREIMS of the diacetate are identical to those for compound **2b**.

4.3.7. Compound (**2d**)

Solid mixture; ^{1}H NMR ($CDCl_3$, 400 MHz) see Table 3 and δ ~1.45 (1H, m, H-1β), 1.17 (1H, dd, H-1α), ~1.58 (2H, m, H-2), 2.28 (1H, brd, H-3β), 1.96 (1H, brq, H-3α), 1.70 (1H, brd, H-5), 1.65 (1H, dq, H-6α), 1.07 (1H, q, H-6β), ~1.43 (1H, tt, H-7), ~1.56 (1H, m, H-8α), ~1.23 (1H, m, H-8β), 1.40 (1H, brd, H-9β), ~1.25 (1H, m, H-9α), 1.17 (3H, s, H-12), 1.21 (3H, s, H-13), 0.66 (3H, s, H-14), 4.67 (1H, brs, H-15a), 4.39 (1H, brs, H-15b), 4.57 (1H, d, H-1'), 4.84 (1H, dd, H-2'), 3.64 (1H, dd, H-3'), 3.70 (1H, dd, H-4'), 3.62 (1H, qd, H-5'), 1.33 (3H, d, H-6'); ^{13}C NMR ($CDCl_3$, 100 MHz) see Table 3. ESI-MS (positive mode): *m/z* 487 $[M+Na]^+$; MS^2 of $[M+Na]^+$: *m/z* 283 $[M+Na-C_{15}H_{24}]^+$. EIMS of the diacetate: *m/z* 548 $[M]^{+\bullet}$ (0.1), 327 $[M-C_{15}H_{25}O]^+$ (14), 204 $[M-C_{15}H_{22}O_8]^{+\bullet}$ (19), 97 (100). HREIMS: *m/z* 548.3339 (calcd for $C_{31}H_{48}O_8$, 548.3349), 327.1445 (calcd for $C_{16}H_{23}O_7$, 327.1444).

4.3.8. Compound (**2e**)

Solid mixture; ^{1}H NMR ($CDCl_3$, 400 MHz) see Table 3 and δ 1.17 (3H, s, H-12), 1.21 (3H, s, H-13), 0.68 (3H, s, H-14), 4.69 (1H, brs, H-15a), 4.42 (1H, brs, H-15b), 4.57 (1H, d, H-1'), 4.81 (1H, dd, H-2'), 1.33 (3H, d, H-6'); ^{13}C NMR ($CDCl_3$, 100 MHz) see Table 3. ESI-MS (positive mode): *m/z* 461 $[M+Na]^+$; MS^2 of $[M+Na]^+$: *m/z* 257 $[M+Na-C_{15}H_{24}]^+$. EIMS of the diacetate: *m/z* 301 $[M-C_{15}H_{25}O]^+$ (15), 204 $[M-C_{15}H_{22}O_8]^{+\bullet}$ (24), 83 (100). HREIMS: *m/z* 301.1293 (calcd for $C_{14}H_{21}O_7$, 301.1287).

4.3.9. Compound (**2f**)

Solid mixture; ^{1}H NMR ($CDCl_3$, 400 MHz) see Table 3 and δ 1.17 (3H, s, H-12), 1.22 (3H, s, H-13), 0.68 (3H, s, H-14), 4.69 (1H, brs, H-15a), 4.42 (1H, brs, H-15b), 4.57 (1H, d, H-1'), 4.82 (1H, dd, H-2'), 3.63 (1H, dd, H-3'), 3.68 (1H, dd, H-4'), 3.61 (1H, qd, H-5'), 1.32 (3H, d, H-6'); ^{13}C NMR ($CDCl_3$, 100 MHz) see Table 3. ESI-MS (positive mode): *m/z* 475 $[M+Na]^+$; MS^2 of

$[M+Na]^+$: *m/z* 271 $[M+Na\text{-}C_{15}H_{24}]^+$. EIMS of the diacetate: *m/z* 315 $[M\text{-}C_{15}H_{25}O]^+$ (15), 204 $[M\text{-}C_{15}H_{22}O_8]^{+\bullet}$ (19), 97 (100). HREIMS: *m/z* 315.1447 (calcd for $C_{15}H_{23}O_7$, 315.1444).

4.3.10. Compound (**3**)

White, amorphous powder; $[\alpha]^{25}_D$ –9.5 (*c* 0.6, isopropanol); ^{1}H NMR ($CDCl_3$, 400 MHz) see Table 1; ^{1}H NMR (CD_3OD, 400 MHz) see Table 1; ^{13}C NMR ($CDCl_3$, 100 MHz) see Table 2. HR-ESI-MS (positive mode): *m/z* 391.2461 $[M+Na]^+$; (calcd. for $C_{21}H_{36}O_5Na$, 391.2455).

4.3.11. Compound (**3d**)

White, amorphous powder; $[\alpha]^{25}_D$ –6.8 (*c* 0.15, $CHCl_3$); ^{1}H NMR ($CDCl_3$, 400 MHz) see Table 1 and δ 5.63 (1H, m, *J* = 1.3 Hz, H-2"), 2.18 (2H, qd, *J* = 7.5, 1.1 Hz, H-4"), 1.08 (3H, t, *J* = 7.5 Hz, H-5"), 2.16 (3H, d, *J* = 1.3 Hz, H-6"); ^{1}H NMR (CD_3OD, 400 MHz) see Table 1 and δ 5.66 (1H, m, H-2"), 2.20 (2H, qd, H-4"), 1.09 (3H, t, H-5"), 2.16 (3H, d, H-6"); ^{13}C NMR ($CDCl_3$, 100 MHz) see Table 2 and δ 166.7 (C, C-1"), 113.6 (CH, C-2"), 163.5 (C, C-3"), 33.9 (CH_2, C-4"), 11.7 (CH_3, C-5"), 18.8 (CH_3, C-6"); ESI-MS (positive mode): *m/z* 487 $[M+Na]^+$; MS^2 of $[M+Na]^+$: *m/z* 283 $[M+Na\text{-}C_{15}H_{24}]^+$; MS^3 of $[M+Na]^+ \rightarrow [M+Na\text{-}C_{15}H_{24}]^+$: *m/z* 265 $[M+Na\text{-}C_{15}H_{24}\text{-}H_2O]^+$. ESI-MS (negative mode): *m/z* 463 $[M-H]^-$; MS^2 of $[M-H]^-$: *m/z* 367 $[M\text{-}H\text{-}C_6H_8O]^-$; MS^3 of $[M-H]^- \rightarrow [M\text{-}H\text{-}C_6H_8O]^-$: *m/z* 145 $[M\text{-}H\text{-}C_6H_8O\text{-}C_{15}H_{26}O]^-$.

4.3.12. Compound (**3a**)

White, amorphous powder; ^{1}H NMR ($CDCl_3$, 400 MHz) δ 1.68 (1H, m, H-5), 0.03 (1H, t, H-6), 0.55 (1H, td, H-7), 0.89 (3H, s, H-12), 0.98 (3H, s, H-13), 1.17 (3H, s, H-14), 0.87 (3H, d, H-15), 4.65 (1H, d, H-1'), 4.98 (1H, dd, H-2'), 3.64 (1H, dd, H-3'), 3.68 (1H, dd, H-4'), 3.61 (1H, qd, H-5'), 1.30 (3H, d, H-6'), 6.13 (1H, qq, *J* = 7.3, 1.4 Hz, H-3"), 2.01 (3H, dq, *J* = 7.3, 1.5 Hz, H-

4"), 1.89 (3H, m, H-5"); ^{1}H NMR (CD_3OD, 400 MHz) δ 1.70 (1H, m, H-5), 0.09 (1H, t, H-6), 0.57 (1H, ddd, H-7), 0.92 (3H, s, H-12), 0.99 (3H, s, H-13), 1.18 (3H, s, H-14), 0.88 (3H, d, H-15), 4.68 (1H, d, H-1'), 5.02 (1H, dd, H-2'), ~3.65 (3H, m, H-3' and H-4' and H-5'), 1.24 (3H, d, H-6'), 6.18 (1H, qq, H-3"), 2.02 (3H, dq, H-4"), 1.90 (3H, m, H-5") ^{13}C NMR ($CDCl_3$, 100 MHz) δ 54.8 (CH, C-1), 82.0 (C, C-10), 94.7 (CH, C-1'), 73.2 (CH, C-2'), 167.8 (C, C-1"), 126.9 (C, C-2"), 139.6 (CH, C-3"), 16.0 (CH_3, C-4"), 20.5 (CH_3, C-5"); ESI-MS (positive mode): *m/z* 473 $[M+Na]^+$; MS^2 of $[M+Na]^+$: *m/z* 269 $[M+Na-C_{15}H_{24}]^+$. EIMS of the diacetate: *m/z* 534 $[M]^{+\bullet}$ (0.4), 313 $[M-C_{15}H_{25}O]^+$ (33), 204 $[M-C_{15}H_{22}O_8]^{+\bullet}$ (85), 83 (100). HREIMS: *m/z* 534.3177 (calcd. for $C_{30}H_{46}O_8$, 534.3193), 313.1285 (calcd. for $C_{15}H_{21}O_7$, 313.1287), 204.1875 (calcd. for $C_{15}H_{24}$, 204.1878).

4.3.13. Compound (**3b**)

Solid mixture; ^{1}H NMR ($CDCl_3$, 400 MHz) δ 0.01 (1H, t, H-6), 0.54 (1H, td, H-7), 0.85 (3H, s, H-12), 0.97 (3H, s, H-13), 1.18 (3H, s, H-14), 0.83 (3H, d, H-15), 4.64 (1H, d, H-1'), 4.98 (1H, dd, H-2'), 1.31 (3H, d, H-6'), 6.87 (1H, qq, J = 7.0, 1.4 Hz, H-3"), 1.79 (3H, dq, J = 7.0, 1.2 Hz, H-4"), 1.83 (3H, m, H-5"); ^{13}C NMR ($CDCl_3$, 100 MHz) δ 81.5 (C, C-10), 94.7 (CH, C-1'), 167.4 (C, C-1"), 128.0 (C, C-2"), 137.6 (CH, C-3"), 14.4 (CH_3, C-4"), 12.1 (CH_3, C-5"). EIMS of the diacetate: *m/z* 534 $[M]^{+\bullet}$ (0.1), 313 $[M-C_{15}H_{25}O]^+$ (0.9), 204 $[M-C_{15}H_{22}O_8]^{+\bullet}$ (2.5), 80 (100). HREIMS: *m/z* 313.1283 (calcd. for $C_{15}H_{21}O_7$, 313.1287), 204.1875 (calcd. for $C_{15}H_{24}$, 204.1878).

4.3.14. Compound (**3c**)

Solid mixture; ^{1}H NMR ($CDCl_3$, 400 MHz) δ 0.03 (1H, t, H-6), 0.55 (1H, td, H-7), 0.84 (3H, s, H-12), 0.97 (3H, s, H-13), 1.18 (3H, s, H-14), 0.87 (3H, d, H-15), 4.61 (1H, d, H-1'), 4.88 (1H, dd, H-2'), 1.31 (3H, d, H-6'), 5.64 (1H, m, J = 1.3 Hz, H-2"), 1.90 (3H, d, J = 1.3 Hz, H-4"), 2.17

(3H, d, J = 1.3 Hz, H-5"); ^{13}C NMR ($CDCl_3$, 100 MHz) δ 81.3 (C, C-10), 95.1 (CH, C-1'), 166.5 (C, C-1"), 115.1 (CH, C-2"), 158.6 (C, C-3"), 27.4 (CH_3, C-4"), 20.2 (CH_3, C-5"). EIMS and HREIMS of the diacetate are identical to those for compound **3b**.

4.3.15. Compound (**3e**)

White, amorphous powder; ^{1}H NMR ($CDCl_3$, 400 MHz) δ 1.73 (1H, m, H-5), 0.06 (1H, t, H-6), 0.57 (1H, td, H-7), 0.94 (3H, s, H-12), 1.00 (3H, s, H-13), 1.17 (3H, s, H-14), 0.91 (3H, d, H-15), 4.60 (1H, d, H-1'), 4.83 (1H, dd, H-2'), 3.58 (1H, dd, H-3'), 3.66 (1H, dd, H-4'), 3.57 (1H, qd, H-5'), 1.30 (3H, d, H-6'), 2.55 (1H, m, J = 7.0 Hz, H-2"), 1.17 (3H, d, J = 7.0 Hz, H-3"), 1.21 (3H, d, J = 7.0 Hz, H-4"); ^{1}H NMR (CD_3OD, 400 MHz) δ ~1.76 (1H, m, H-5), 0.12 (1H, t, H-6), 0.59 (1H, ddd, H-7), 0.96 (3H, s, H-12), 1.01 (3H, s, H-13), 1.18 (3H, s, H-14), 0.92 (3H, d, H-15), 4.64 (1H, d, H-1'), 4.94 (1H, dd, H-2'), ~3.62 (3H, m, H-3' and H-4' and H-5'), 1.23 (3H, d, H-6'), 2.54 (1H, m, H-2"), 1.16 (3H, d, H-3"), 1.20 (3H, d, H-4"); ^{13}C NMR ($CDCl_3$, 100 MHz) δ 55.1 (CH, C-1), 82.1 (C, C-10), 94.6 (CH, C-1'), 73.6 (CH, C-2'), 177.6 (C, C-1"), 34.1 (CH, C-2"), 18.5 (CH_3, C-3"), 19.6 (CH_3, C-4"); ESI-MS (positive mode): m/z 461 $[M+Na]^+$; MS^2 of $[M+Na]^+$: m/z 257 $[M+Na\text{-}C_{15}H_{24}]^+$.

4.4. Basic hydrolysis

A portion of the crude fraction H from FC (~50 mg) was dissolved in MeOH (2.5 mL), mixed to a soln. of KOH (1 M, 2.5 mL) in a round bottomed flask and stirred at 40 °C for 20 h. After cooling at room temperature, the solution was neutralized with formic acid (~ 0.25 mL). RP18 gel for FC (1 spoon) was added to the clear solution and the solvent was evaporated. The desiccated slurry was applied to a short FC column packed with RP18, washed with water and eluted with methanol. The solvent was finally evaporated to give the sesquiterpene glycosides

mixture (~40 mg) that was purified by reversed phase HPLC. The eluents were MeOH−H_2O (75:25) and the detection wavelength was set at 210 nm. Three main fractions were collected that contained the compounds **1** (t_R=13.1 min, mg 6.7), **2** (t_R=15.5 min, mg 14.5) and **3** (t_R=21.1 min, mg 9.2).

4.5. Acid hydrolysis

The acidic hydrolysis of sesquiterpene glycosides was carried out by a microwave-assisted method (Xiping and Yangde, 2008). A portion of the saponified mixture was dissolved in a solution prepared with 1.4 mL of *i*-PrOH−H_2O (50:50) and 0.28 mL of concentrated HCl (36%) that was transferred in a microwave vessel and placed on the turntable of the microwave oven. Hydrolysis progressed for 2 min using 300 W of microwave radiation power at the temperature 80 ºC. The reaction mixture was then neutralized with aqueous Na_2CO_3 (0.35 g in 5 mL), transferred to a separating funnel and repeatedly extracted with *n*-hexane. The polar phase was concentrated and purified by prep. TLC ($CHCl_3$−MeOH−H_2O, 60:34:6) to give pure fucose (R_f=0.32, 15 mg). The sugar was identified by its proton NMR spectra and gave a specific optical rotation ($[\alpha]_D$ = +22.7 (*c* = 0.79, water)) which is consistent with the D-enantiomer.

4.6. Acetylation

The compounds **1a**, **2a**, **2b**+**2c**+**2e**, **2d**+**2f**, **3a**, **3b**+**3c** and **3d** were subjected to esterification of the hydroxyls HO-3' and HO-4'. Dry pyridine (20μL) and acetic anhydride (20μL) were added under nitrogen to each sample (~0.4 mg) in a small screw-capped vial. The solution was allowed to stand at room temperature for 2 days and then evaporated. The residue was dissolved in methanol and analyzed by EI-MS without any preliminary purification. Only the diacetate products could be detected. The abundant compounds **1a**, **2a** and **3d** were also investigated by

NMR spectroscopy thus revealing that the yield of acetylation was nearly quantitative without any detectable by-product.

4.6.1. Diacetate of compound (**1a**):

^{1}H NMR ($CDCl_3$, 400 MHz) δ 5.78 (1H, dd, J = 17.8, 10.6 Hz, H-1), 4.87 (2H, m, H-2), 4.78 (1H, m, H-3a), 4.55 (1H, brs, H-3b), 1.13 (3H, s, H-12), 1.21 (3H, s, H-13), 0.95 (3H, s, H-14), 1.68 (3H, brs, H-15), 4.66 (1H, d, J = 7.8 Hz, H-1'), 5.28 (1H, dd, J = 7.8, 10.3 Hz, H-2'), 5.11 (1H, dd, J = 10.3, 3.4 Hz, H-3'), 5.22 (1H, dd, J = 3.4, 1.1 Hz, H-4'), 3.79 (1H, qd, J = 1.1, 6.4 Hz, H-5'), 1.20 (3H, d, J = 6.4 Hz, H-6'), 6.07 (1H, qq, J = 7.3, 1.5 Hz, H-3''), 1.95 (3H, dq, J = 7.3, 1.5 Hz, H-4''), 1.83 (3H, qd, J = 1.5 Hz, H-5''), 2.16 (3H, s, AcO-4'), 1.94 (3H, s, AcO-3'). EIMS: m/z 534 $[M]^{+\bullet}$ (0.1), 313 $[M\text{-}C_{15}H_{25}O]^+$ (11), 204 $[M\text{-}C_{15}H_{22}O_8]^{+\bullet}$ (18), 83 (100). HREIMS: m/z 534.3187 (calcd. for $C_{30}H_{46}O_8$, 534.3192), 476.2782 (calcd. for $C_{27}H_{40}O_7$, 476.2774), 313.1284 (calcd. for $C_{15}H_{21}O_7$, 313.1287), 204.1873 (calcd. for $C_{15}H_{24}$, 204.1878).

4.6.2. Diacetate of compound (**2a**):

^{1}H NMR ($CDCl_3$, 400 MHz) δ ~2.28 (1H, brd, H-3β), 1.12 (3H, s, H-12), 1.20 (3H, s, H-13), 0.66 (3H, s, H-14), 4.68 (1H, brs, H-15a), 4.43 (1H, brs, H-15b), 4.67 (1H, d, J = 7.8 Hz, H-1'), 5.29 (1H, dd, J = 7.8, 10.4 Hz, H-2'), 5.11 (1H, dd, J = 10.4, 3.5 Hz, H-3'), 5.22 (1H, dd, J = 3.5, 1.1 Hz, H-4'), 3.78 (1H, qd, J = 1.1, 6.4 Hz, H-5'), 1.19 (3H, d, J = 6.4 Hz, H-6'), 6.07 (1H, qq, J = 7.3, 1.5 Hz, H-3''), 1.96 (3H, dq, J = 7.3, 1.5 Hz, H-4''), 1.84 (3H, qd, J = 1.5 Hz, H-5''), 2.17 (3H, s, AcO-4'), 1.95 (3H, s, AcO-3'). EIMS: m/z 534 $[M]^{+\bullet}$ (0.1), 313 $[M\text{-}C_{15}H_{25}O]^+$ (1.2), 204 $[M\text{-}C_{15}H_{22}O_8]^{+\bullet}$ (1.5), 80 (100). HREIMS: m/z 534.3184 (calcd. for $C_{30}H_{46}O_8$, 534.3193), 313.1285 (calcd. for $C_{15}H_{21}O_7$, 313.1287), 204.1880 (calcd. for $C_{15}H_{24}$, 204.1878).

4.6.3. Diacetate of compound (**3d**):

^{1}H NMR ($CDCl_3$, 400 MHz) δ 0.02 (1H, t, J = 9.5 Hz, H-6), 0.55 (1H, td, J = 9.5, 9.5, 7.6 Hz, H-7), 0.83 (3H, s, H-12), 0.96 (3H, s, H-13), 1.17 (3H, s, H-14), 0.83 (3H, d, J = 6.7 Hz, H-15), 4.69 (1H, d, J = 8.0 Hz, H-1'), 5.24 (1H, dd, J = 8.0, 10.4 Hz, H-2'), 5.02 (1H, dd, J = 10.4, 3.5 Hz, H-3'), 5.20 (1H, dd, J = 3.5, 1.1 Hz, H-4'), 3.74 (1H, qd, J = 1.1, 6.4 Hz, H-5'), 1.18 (3H, d, J = 6.4 Hz, H-6'), 5.54 (1H, tq, J = 1.3 Hz, H-2''), 2.16 (2H, qd, H-4''), 1.06 (3H, t, J = 7.5 Hz, H-5''), 2.14 (3H, d, J = 1.3 Hz, H-6''), 2.16 (3H, s, AcO-4'), 1.94 (3H, s, AcO-3'). EIMS of the diacetate: *m*/*z* 548 $[M]^{+\bullet}$ (0.1), 327 $[M\text{-}C_{15}H_{25}O]^+$ (15), 204 $[M\text{-}C_{15}H_{22}O_8]^{+\bullet}$ (94), 97 (100). HREIMS: *m*/*z* 327.1438 (calcd. for $C_{16}H_{23}O_7$, 327.1444), 204.1876 (calcd. for $C_{15}H_{24}$, 204.1878).

4.7. Cytotoxicity assays

Cytotoxicity of fractions and individual compounds was performed in human epithelial gastric cells AGS by MTT assay and LDH release. For MTT assay, cells were treated with fractions (10 µg/mL) or individual molecules (5-20 µM) for 24 h; the final concentration of the vehicle (DMSO) was 0.2%. Then, growth media were removed and 200 µL of phosphate-buffered saline (PBS) containing MTT, at a final concentration of 0.1 mg/mL, was added to each well. After 1 h incubation at 37 °C, MTT dye was removed and 200 µL/well of extracting solution (*i*-PrOH−DMSO, 9:1) was added. Absorbance was measured on a microplate reader at 550 nm. Cells treated with Triton-X100 1% for 24 h were used as positive control (around 100% inhibition of cell viability). Treatment effects on cellular viability were expressed by setting the percentage of cells treated only with this vehicle at 100%. LDH release was measured with the LDH Cytotoxicity Detection Kit (Takara Bio Inc.) following the manufacturer's instructions. Briefly, 24 h after treatment with compounds (final concentration of DMSO was 0.2%), samples were centrifuged, and 100 µL of medium of each well was added to 100 µL of a reaction mixture

containing a catalyst and a dye solution. Samples were incubated for 15 minutes at room temperature, and LDH activity was quantified measuring the absorbance at 490 nm on a microplate reader. A medium of AGS cells treated with Triton-X100 1% for 24 h was used as a positive control (around 90% inhibition of cell viability). Cytotoxicity of fractions (5-20 μg/mL) and individual compounds (5-20 μM) was calculated as a percentage, setting the control viability treated only with the vehicle at 100%. Experiments, including those used to calculate IC_{50}, were performed three times in triplicate and the average values ± S.D. were reported.

4.8. In vitro digestion of CH_2Cl_2 extract

Gastric digestion was simulated using a protocol previously described, with minor modifications (Oomen et al., 2003; Versantvoort et al., 2005). Briefly, CH_2Cl_2 extract (60 mg) was incubated for 5 min at 37 °C with 0.6 mL of saliva juice (12 mM KCl, 2 mM KSCN, 7.4mM NaH_2PO_4, 4 mM Na_2SO_4, 5 mM NaCl, 1.8 mM NaOH, 3.3 mM urea, 89 μM uric acid, 145 mg/L amylase and 50 mg/L mucin). Then 1.2 mL of gastric juice (47 mM NaCl, 2.2 mM NaH_2PO_4, 11 mM KCl, 2.7 mM $CaCl_2$, 5.7 mM NH_4Cl, 8.3 mL/L HCl, 3.6 mM glucose, 0.1 mM glucuronic acid, 1.4 mM urea, 1.5 mM glucosaminehydrochloride, 1 g/L BSA, 1 g/L pepsin and 3 g/L mucin) was added to the suspension and the sample was incubated for 2 h at 37°C. At the end of the incubation, the digested sample was frozen and lyophilized. The crude extract and lyophilized mixture were dissolved in methanol and then analyzed by HPLC over the Luna CN column: the chromatographic profiles were quite similar particularly in the region where the sesquiterpene glycosides were eluted. This suggests that sesquiterpene glycosides are unaffected by the *in vitro* digestive treatment.

Acknowledgements

We gratefully acknowledge the excellent technical assistance of Mr Sandro Gadotti and dr. Paola Montoro for generously supplying HRESIMS data. This work was financially supported by MIUR and by “Piano di Sviluppo UNIMI-linea B”. The fellowship of Alexandru Ciocarlan was partially funded by Provincia Autonoma di Trento, Project "PARMA" (Piante Alimentari aRomatiche e Medicinali Alpine), no. 1587; the fellowship of Elisa Colombo was partially funded by FSE, Regione Lombardia.

Appendix A. Supplementary data

Supplementary data associated with this article can be found, in the online version, at

References

Abdel-Mogib, M.; Jakupovic, J.; Dawidar, A. M., 1989. 10-*epi*-Cubebolxyloside from *Iphiona scabra*. Phytochemistry 28, 2202-2203.

Andersen, F.A.; Bergfeld, W.F.; Belsito, D.V.; Hill, R.A.; Klaassen, C.D.; Liebler, D.C.; Marks, J.G., Jr; Shank, R.C.; Slaga, T.J.; Snyder, P.W. Final Report of the Cosmetic Ingredient Review Expert Panel Amended Safety Assessment of *Calendula officinalis* - Derived Cosmetic Ingredients. International Journal of Toxicology 2010, 29, 221S-243S.

Campanini, E., 2003. Dizionario di Fitoterapia e Piante Medicinali, Editore Tecniche Nuove, Milano.

Cravotto, G., Boffa, L., Genzini, L., Garella, D., 2010. Phytotherapeutics: an evaluation of the potential of 1000 plants. J. Clin. Pharm. Ther. 35, 11-48.

De Tommasi, N., Pizza, C., Conti, C., Orsi, N., Stein, M.L., 1990. Structure and in vitro antiviral activity of sesquiterpene glycosides from *Calendula arvensis*. J. Nat. Prod. 53, 830-835.

Dulf, F.V., Pamfil, D., Baciu, A.D., Pintea, A., 2013. Fatty acid composition of lipids in pot marigold (*Calendula officinalis* L.) seed genotypes. Chem. Cent. J. 7, 8.

Fletcher, M.T., Lowe, L.M., Kitching, W., König, W.A., 2000. Chemistry of leichhardt's grasshopper, *Petasida ephippigera*, and its host plants, *Pityrodia jamesii*, *P. ternifolia*, and *P. pungens*. J. Chem. Ecol. 26, 2275-2290.

Fotakis, G., Timbrell J.A., 2006. In vitro cytotoxicity assays: comparison of LDH, neutral red, MTT and protein assay in hepatoma cell lines following exposure to cadmium chloride. Toxicol. Lett. 160, 171-177.

Freeman, F., Hwang, J.H., Junge, E.H., Parmar, P.D., Renz, Z., Trinh J., 2008. Conformational analysis of cycloheptane, oxacycloheptane, 1,2-dioxacycloheptane, 1,3-dioxacycloheptane, and 1,4-dioxacycloheptane. Int. J. Quantum Chem. 108, 339-350.

Hirota, H., Tomono, Y., Fusetani, N., 1996. Terpenoids with antifouling activity against Barnacle larvae from the marine sponge *Acanthella cavernosa*. Tetrahedron 52, 2359-2368.

Jakupovic, J., Grenz, M., Bohlmann, F., Rustaiyan, A., Koussari, S., 1988. Sesquiterpene glycosides from *Calendula persica*. Planta Med. 54, 254-256.

Jolad, S.D., Timmermann, B.N., Hoffmann, J.J., Bates, R.B., Camou, F.A., Siahaan, T.J., 1988. Sesquiterpenoid glycosides and an acetogenin glucoside from *Lessingia glandulifera*. Phytochemistry 27, 2199-2204.

Kaplan, M.A.C., Pugialli, H. R. L., Lopes, D., Gottlieb, H. E., 2000. The stereochemistry of ledol from *Renealmia chrysotrycha*: an NMR study. Phytochemistry 53, 749-753.

Kaškonienė, V., Kaškonas, P., Jalinskaitė, M., Maruška, A., 2011. Chemical composition and chemometric analysis of variation in essential oils of *Calendula officinalis* L. during vegetation stages. Chromatographia 73, 163-169.

Kingston, D.G.I., Rao, M.M., Spittler, T.D., Pettersen, R.C., Cullen, D.L., 1975. Sesquiterpenes from *Flourensia cernua*. Phytochemistry 1975, 14, 2033-2037.

Kishimoto, S., Ohmiya, A., 2009. Studies on carotenoids in the petals of compositae plants. J. Japan. Soc. Hort. Sci. 78, 263-272.

Marukami, T., Kishi, A., Yoshikawa, M., 2001. Medicinal Flowers. IV. Marigold. (2): structures of new ionone and sesquiterpene glycosides from egyptian *Calendula officinalis*. Chem. Pharm. Bull. 49, 974-978.

Muley, B.P., Khadabadi, S.S., Banarase, N.B., 2009. Phytochemical constituents and pharmacological activities of *Calendula officinalis* Linn (Asteraceae): a review. Trop. J. Pharm. Res. 8, 455-465.

Neukirch, H., D'Ambrosio, M., Dalla Via, J., Guerriero, A., 2004. Simultaneous quantitative determination of eight triterpenoid monoesters from flowers of 10 varieties of *Calendula officinalis* L. and characterisation of a new triterpenoid monoester. Phytochem. Anal. 15, 30-35.

Neukirch, H., D'Ambrosio, M., Sosa, S., Altinier, G., Della Loggia, R., Guerriero, A., 2005. Improved anti-inflammatory activity of three new terpenoids derived, by systematic chemical modifications, from the abundant triterpenes of the flowery plant *Calendula officinalis*. Chem. Biodivers. 2, 657-671.

Oomen, A.G.; Rompelberg, C.J.; Bruil, M.A.; Dobbe, C.J.; Pereboom, D.P.; Sips, A.J., 2003. Development of an *in vitro* digestion model for estimating the bioaccessibility of soil contaminants Arch. Environ. Contam. Toxicol. 44, 281-287.

Pettersen, R.C., Cullen, D.L., Spittler, T.D., Kingston, D.G.I, 1975. The crystal and molecular structure of flourensadiol, a natural product sesquiterpene isolated from a west Texas shrub. Acta Cryst. B31, 1124-1127.

Pizza, C., De Tommasi, N., 1988. Sesquiterpene glycosides based on the alloaromadendrane skeleton from *Calendula arvensis*. Phytochemistry 27, 2205-2208.

Singh, M.K., Sahu, P., Nagori, K., Dewangan, D., Kumar, T., Alexander, A., Badwaik, H., Tripathi, D.K., 2011. Organoleptic properties in-vitro and in-vivo pharmacological activities of *Calendula officinalis* Linn: an over review. J. Chem. Pharm. Res. 3, 655-663.

Szakiel, A., Ruszkowski, D., Janiszowska, W., 2005. Saponins in *Calendula officinalis* L. – structure, biosynthesis, transport and biological activity. Phytochemistry Reviews 4, 151-158.

Takaoka, D., Kawahara, H., Ochi, S., Hiroi, M., Nozaki, H., Nakayama, M., Ishizaki, K., Sakata, K., Ina, K., 1986. The structures of sesquiterpene glycosides from *Pittosporum tobira* Ait. Chem. Lett. 1121-1124.

Thamapipol, S., Kündig, E.P., 2011. Intramolecular Diels-Alder reactions using chiral ruthenium Lewis acids and application in the total synthesis of *ent*-ledol. Org. Biomol. Chem. 9, 7564-7570.

Versantvoort, C.H.; Oomen, A.G.; Van de Kamp, E.; Rompelberg, C.J.; Sips, A., 2005. Applicability of an in vitro digestion model in assessing the bioaccessibility of mycotoxins from food. J. Food Chem. Toxicol. 43, 31-40.

Xiping Chen, J., Yangde Zhang Y., 2008. Rapid microwave-assisted hydrolysis for determination of ginkgo flavonol glycosides in extracts of *Ginkgo biloba* leaves. J. Chromatogr. Sci. 46, 117-121.

Yoshikawa, M., Marukami, T., Kishi, A., Kageura, T., Matsuda, H., 2001. Medicinal Flowers. III. Marigold. (1): hypoglycemic, gastric emptying inhibitory, and gastroprotective principles and new oleanane-type triterpene oligoglycosides, calendasaponins A, B, C, and D, from egyptian *Calendula officinalis*. Chem. Pharm. Bull. 49, 863-870.